*Article*

# Black Widow Optimization Algorithm Used to Extract the Parameters of Photovoltaic Cells and Panels

**Manoharan Madhiarasan** [ID], **Daniel T. Cotfas** *[ID] **and Petru A. Cotfas** [ID]

Department of Electronics and Computers, Faculty of Electrical Engineering and Computer Science, Transilvania University of Brasov, 500036 Brasov, Romania
* Correspondence: dtcotfas@unitbv.ro

**Abstract:** The metaheuristic algorithms and their hybridization have been utilized successfully in the past to extract the parameters of photovoltaic (PV) cells and panels. The novelty of the paper consists of proposing the black widow optimization algorithm (BWOA) for the first time to identify the parameters of the two photovoltaic cells RTC France, amorphous silicon (aSi), and two photovoltaic panels PWP201, PVM 752 GaAs. The single-diode model (SDM) and double-diode model (DDM) for analyzing the PVs are considered. The performance of the BWOA is verified using four statistical tests: the root mean square error, which is the primary tool, the mean relative error, the mean bias error, and the coefficient of determination. The research results of this study are as follows: BWOA gave the same results, or very slightly better, for RTC and PWP201 for SDM in comparison with the best algorithms from the specialized literature; for all the other cases, BWOA has substantially better results, especially for PVM 752 GaAs, where the improvements in RMSE are: 16.5%, for PWP201: 6.25%, and for aSi: 5.3%, all for the DDM; the computing time is around 2 s, which is one of the lowest durations. A consistent study is made to optimize the accuracy and computational time in function of the number of iterations and population.

**Keywords:** optimization algorithm; photovoltaic; extraction; parameters; modeling

**MSC:** 90C31; 68W40; 68U35

## 1. Introduction

The contemporary energetic crisis creates high pressure on power plants and energy prices. This can be a very good opportunity for the development and increase in the capacities of installed photovoltaics, similarly to the last crises, starting with the crisis in the 1970s. Additionally, there is the European Union program for climate neutrality by 2050 [1]. This target can be reached if very good photovoltaic cells are used and connected efficiently [2], alongside smart photovoltaic systems [3].

The best panels are obtained using the twin photovoltaic cells. This goal can be obtained if the photovoltaic cells are measured accurately for the production process in a very short time.

The extraction of the photovoltaic cell/panel parameters can be made using analytic methods and metaheuristic algorithms. The current-voltage characteristic, and the mathematical model based on the equivalent circuit are essential tools for analyzing photovoltaic cells and panels. Cotfas et al. analyzed the pros and cons of 33 analytical methods [4]. Humada et al. have chosen and discussed five analytic methods for each group considered. The first group is for five parameters, the next for four, three, two, and the last is for one [5]. These methods have both advantages and disadvantages. One of the important advantages is the very short time necessary for extraction, which is very useful for industry, but it comes with a significant drawback, namely the reduction in accuracy, important for research [6]. In recent years, after 2000, a new approach was taken using metaheuristic algorithms, which are very useful for optimization problems, especially for multimodal

issues, such as photovoltaic cells parameters extraction. Today, the number of metaheuristic algorithms surpasses that of analytical methods, and in the near future, this will increase due to a large number of algorithms developed for different purposes. These algorithms can be applied to the photovoltaic parameters extraction problem. There are several review papers that analyzed the articles where the metaheuristic algorithms are presented. Yang et al. considered four groups for the metaheuristic algorithms: sociology algorithms, mathematics algorithms, physics algorithms, and biology algorithms [7]. Li et al. analyzed the metaheuristic algorithms from the point of view of computational time, resources, and statistical tests [8].

The main statistical test to analyze the performance of the algorithms is the root mean square error (RMSE) [7,9]. The algorithms with the lowest RMSE from each group are chosen for comparison with the BWOA. This choice is made for the RTC photovoltaic cell and PWP 201 photovoltaic panel, whose datasets are the most commonly used in the specialized literature. In the cases when these metaheuristic algorithms are not applied to extract parameters, they are replaced with others. These new algorithms must give very good values for the RMSE, namely the lowest ones.

The biology group is the most populated; Yang et al. briefly described 14 algorithms [7]. The algorithm chosen from this group is the improved whale optimization algorithm (IWOA). This algorithm has the best RMSE results in comparison with the others from the biology group for both models, which describe the photovoltaic cells using the one diode model (SDM) and two diode model (DDM). It is the improved version of the whale optimization algorithm that is based on the hunting mechanism of humpback whales [10]. From the physics group, the following algorithm is used for comparison—improved Lozi map-based chaotic optimization algorithm (ILCOA). Its performance derives from its ability to search the global optimum in the whole space [11]. The multiple learning backtracking search algorithm (MLBSA) [12] is part of the sociology group. It is an improved version of the backtracking search algorithm proposed by Civicioglu [13]. The performance is due to finding the equilibrium between the exploration and exploitation abilities. This led to an increase in the performance and the convergence speed. The improved shuffled complex evolution algorithm (ISCE) is one of the chosen algorithms from the mathematic group. The RMSE results are among the best for some PV devices, and it has an advantage in comparison with other algorithms; it needs a small number of iterations [14,15]. The second algorithm from the mathematic group is an improved version of the successive discretization algorithm (SDA) [16]. HSDA is a hybrid algorithm that uses the SDA algorithm on the vicinities created around the solutions given by one of the known algorithms [9]. The other utilized algorithms are: barnacle mating optimizer algorithm (BMOA), which is based on the mating behavior of barnacles and belongs to the biology group [17]; guaranteed convergence particle swarm optimization algorithm (GCPSO), which pertains to the physics group and has the very important advantage of avoiding premature convergence [18]; evaporation rate-based water cycle algorithm (ER-WCA), from the physics group and based on the water cycle process in nature [19], having an improved convergence for the global minimum and high accuracy; supply-demand-based optimization algorithm (SDO) [20], based on the economic cobweb model which makes the correspondence between the convergent mode with the exploitation, the divergent mode with the exploitation, and the closed mode with demarcation; enhanced Harris hawks optimization (EHHO), is an improved version of the Harris hawks optimization using general opposition-based learning and orthogonal learning [21].

Table 1 presents a picture of the algorithms applied to extract the parameters of the photovoltaic cells and panels with pros and cons. Additionally, new algorithms with high and good results are added, such as: honey badger algorithm with oppositional-based learning (HBA-OBL) [22], African vultures optimization algorithm (AVOA) [23], improved slime mold optimizer (ImSMA) [24], genetic algorithm with convex combination crossover (GACCC) [25], niche particle swarm optimization in parallel computing (NPSOPC) [26],

enhanced adaptive differential evolution algorithm (EJADE) [27], neural network algorithm with reinforcement learning (RLNNA) [28].

**Table 1.** Literature review of recent optimization algorithms.

| Algorithm | Pros | Cons | Statistical Tests | Year |
|---|---|---|---|---|
| IWOA [10] | • Fast convergence; good robustness<br>• Avoid trapping into local minimum and find the global minimum; good accuracy | • Sensitive parameter setting | RMSE; SIAE; Wilcoxon's test | 2018 |
| ILCOA [11] | • High accuracy<br>• High convergence rate | • Poor stability and robustness<br>• Possibility to remain in the local minimum | RMSE; MAE; NMAE; MBE | 2019 |
| MLBSA [7,12] | • High accuracy: the speed of convergence<br>• A proper balance between local and global exploitation | • Poor search accuracy and reliability in the absence of an elite mechanism based on chaotic local search<br>• High computational time | RMSE | 2018 |
| ISCE [14] | • Finding global minimum<br>• High accuracy; good robustness<br>• The number of iterations is small | • Few statistical tests | RMSE | 2018 |
| HSDA [9] | • High accuracy<br>• Strong global searching capacity | • High computational time | RMSE; MAE; t-statistic; MBE; R2 | 2021 |
| BMOA [17] | • Good accuracy and reliability<br>• The number of iterations is small | • Medium computational time | RMSE; MSE; MAPE; MBE; MAE; MRE | 2022 |
| GCPSO [18] | • Avoids premature convergence<br>• Few adjustable parameters<br>• High convergence performance | • Convergence is guaranteed, but this can be local or global minimum | RMSE; MAE; SSE; ξ | 2018 |
| ER-WCA [19] | • Fast convergence<br>• A proper balance between local and global exploration | • Medium solution quality | RMSE; MAE; MRE | 2017 |
| SDO [20] | • Ability to balance exploration and exploitation<br>• Good accuracy for SDM model; good convergence | • Medium solution quality | RMSE; SIAE; Wilcoxon's test | 2019 |
| EHHO [21] | • Good accuracy and reliability | • Medium solution quality, especially for DDM | RMSE; RE | 2020 |
| HBA-OBL [22] | • Good accuracy<br>• High convergence | • Few statistical tests | RMSE; RE | 2022 |

**Table 1.** *Cont.*

| Algorithm | Pros | Cons | Statistical Tests | Year |
|---|---|---|---|---|
| AVOA [23] | • Low computational complexity<br>• Prevents premature convergence | • Medium execution time | Wilcoxon rank-sum test | 2021 |
| ImSMA [24] | • Good balance between the exploration and exploitation | • Medium solution quality<br>• Few statistical tests | RMSE | 2021 |
| GACCC [25] | • A proper balance between finding good solutions and diversification of the search space<br>• Good accuracy | • Few statistical tests | RMSE | 2017 |
| NPSOPC [26] | • Good global optimal searchability. | • Medium solution quality<br>• Few statistical tests | RMSE | 2020 |
| EJADE [27] | • Good convergence speed<br>• Good balance of exploration and exploitation in the process of evolution | • The number of iterations is high<br>• Medium execution time | RMSE | 2020 |
| RLNNA [28] | • Good accuracy<br>• High stability | • High execution time<br>• Medium computational complexity | RMSE; Wilcoxon test | 2021 |

MAE—mean absolute error; SIAE—sum of individual absolute error; NMAE—normalized MAE; SSE—sum squared error, ξ—weighted RMSE proposed; RE—relative error.

The paper aims to address several research questions, which are listed below:

- Why is the photovoltaic cell or panel parameter extraction needed?
- What are the limitations of analytic methods in extracting the photovoltaic cell parameters?
- Why are metaheuristic algorithms used for photovoltaic cell or panel parameter extraction?
- Can the results previously obtained by other research be further improved using novel algorithms?

New metaheuristic algorithms are developed by researchers to solve the global optimization problems for all groups previously mentioned. These new algorithms can be adapted to solve the problem of photovoltaic cells and panels parameters determination which is a multimodal one. Zamani et al. classified metaheuristic algorithms into single solution and population-based ones. For the last group, the swarm algorithms are classified according to the years and behaviors of diverse species in the following subgroups: insects, terrestrial animals, birds, and aquatic animals, which include the new algorithms [29]. In addition, new metaheuristic algorithms are classified in [30], where the groups are: physics—containing both physical and mathematical concepts in nature, swarm, and evolutionary. For the evolutionary subgroup, the differential evolution algorithms are widely discussed. From the new metaheuristic algorithms, the BWOA is chosen for usage to extract the parameters of the photovoltaic cells and panels.

The main target of this paper is to improve the determination of the photovoltaic cells and panels parameters and to reduce the computational time using the black widow optimization algorithm. Two versions of the black widow optimization algorithm: pheromone

value BWOA and cannibalism BWOA are used for RTC (both models) and PWP201 (both models), but without very good results [31]. The novelty and contributions of this paper are:

- The black widow optimization algorithm is adapted and used for the first time in order to estimate the parameters of the photovoltaic cells and panels (amorphous silicon (aSi) and PVM 752 GaAs) for the single diode and double model;
- The results obtained for the photovoltaic cell and panels parameters using BWOA are compared with the ones given by the best metaheuristic models from the specialized literature, using four statistical tests, such as the root mean square error (RMSE), mean relative error (MRE), the mean bias error (MBE), the coefficient of determination $R^2$ and adjusted coefficient of determination $R_a{}^2$;
- Analyzing the RMSE when the number of the iterations and population vary so as to identify the best solution;
- The results obtained by BWOA prove the superiority or equality in performance with the best metaheuristic algorithms. The best improvement is by 16.5% for the PVM 752 GaAs in the case of the two diodes model;
- The accuracy in determining the photovoltaic cells and panels parameters and the computational time are significantly improved.

The paper is structured as follows: models of the photovoltaic cells and panels and statistical tests are given in Section 2, the results and discussions are presented in Section 3, and in Section 4, the conclusions and the future work are presented.

## 2. Methods

The current-voltage characteristic is the tool used to extract the photovoltaic cells and panels parameters [4]. The short circuit current, open circuit voltage, and maximum power can be obtained directly from the current-voltage characteristic. Other parameters: $I_{ph}$—the photogenerated current, $I_0$—the reverse saturation current, $R_s$ and $R_{sh}$, the parasitic resistance series and shunt, and n—the ideality factor of the diode can be obtained using the different methods and algorithms discussed before. All current-voltage characteristics used in the paper as datasets are measured. There are more techniques for this, such as the capacitor, the potentiometer, and MOSFET techniques [32]. The BWOA is proposed to extract the parameters of two photovoltaic cells and two photovoltaic panels, using both models SDM and DDM.

### 2.1. Models

The behavior of the photovoltaic cells and panels is described using equivalent circuits and mathematical models. Equation (1) represents the mathematical DDM model of the photovoltaic panel with $N_s$ cells connected in series [27]. The first bracket multiplied with $I_{01}$ is the $I_{d1}$, and the second multiplied with $I_{02}$ is $I_{d2}$. The model for the photovoltaic cell is obtained using Equation (1), $N_s$ equal to 1. The SDM model is obtained from Equation (1) if the second bracket is 0. For the DDM model, index 1 and 2 represent the diffusion mechanism and generation-recombination mechanism, respectively.

$$I = I_{ph} - I_{01}\left(e^{\frac{V+N_sIR_s}{n_1N_sV_T}} - 1\right) - I_{02}\left(e^{\frac{V+N_sIR_s}{n_2N_sV_T}} - 1\right) - \frac{V+N_sIR_s}{N_sR_{sh}} \tag{1}$$

The thermal voltage $V_T$ = kT/q is calculated for all photovoltaic cells and panels, using the following values for Boltzmann constant—$k = 1.3806503 \times 10^{-23}$ J/K and for the elementary electrical charge—$q = 1.6021766 \times 10^{-19}$ C.

The equivalent circuit of the photovoltaic cell for the SDM model is presented in Figure 1a, where the diode, $R_{sh}$ and the current source are bound in parallel. DDM model is presented in Figure 1b, in this case the current source, two diodes and $R_{sh}$ are in parallel.
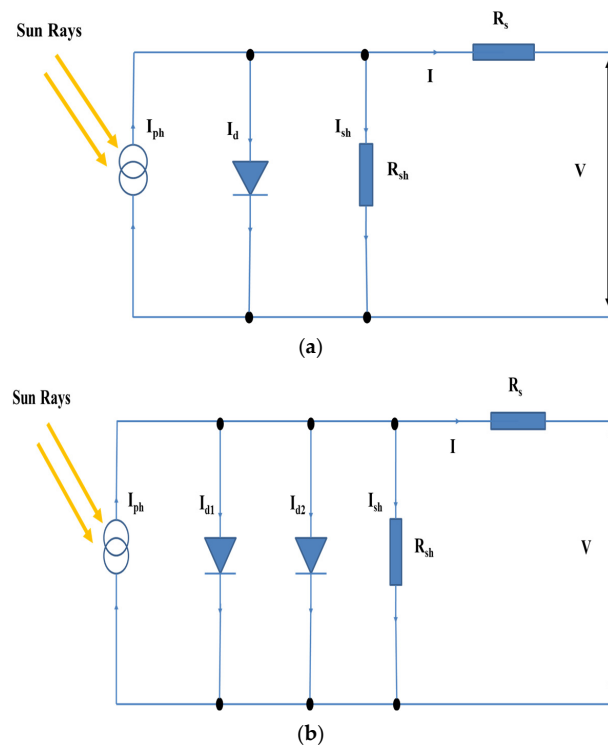
**Figure 1.** Equivalent circuits of the photovoltaic cell: (**a**) SDM model; (**b**) DDM model.

*2.2. Statistical Tests*

Five statistical tests are used to analyze the performance of the BWOA. These tests are the root mean square error, Equation (2), the mean relative error, Equation (3), the mean bias error, Equation (4), the coefficient of determination, Equation (5), and adjusted coefficient of determination, Equation (6).

$$RMSE_{(I,V)} = \sqrt{\frac{\sum\limits_{i=1}^{p} (I_{ic} - I_{im})^2}{p}} \tag{2}$$

$$MRE_{(I,V)} = \frac{\sum\limits_{i=1}^{p} \left| \frac{(I_{ic} - I_{im})}{\overline{I}_{im}} \right|}{p} \tag{3}$$

$$MBE_{(I,V)} = \frac{\sum\limits_{i=1}^{p} (I_{ic} - I_{im})}{p} \tag{4}$$

$$R^2 = 1 - \frac{\sum\limits_{i=1}^{p} (I_{ic} - I_{im})^2}{\sum\limits_{i=1}^{p} \left( I_{im} - \overline{I_{im}} \right)^2} \tag{5}$$

$$R_a^2 = 1 - \frac{p-1}{p-k-1} \left( 1 - R^2 \right) \tag{6}$$

where $p$ represents the number of measurement points, $I_{ic}$ is the computed current, $I_{im}$ is the measured current, $\overline{I}_{im}$ is the average of the measured current, and k represents the number of parameters.

The objective function in this study is to minimize the root mean square error $RMSE_{(x)}$, where $x$ represents the five or seven parameters used for the SDM model and DDM model, respectively.

### 2.3. Black Widow Optimization Algorithm

Hayyolalam and Kazem [33] developed a black widow optimization algorithm, based on inspiration from black widow spider mating behavior. Peña-Delgado et al. [34] used the black widow optimization algorithm in a three-phase eleven-level inverter for selective harmonic elimination. The male of the black widow spider actively assists the female in sexual cannibalism. Devotion during mating has increased the likelihood of more eggs being fertilized. Cannibalism is commonly associated with demography and has significant population-level implications. Cannibalism is a unique stage in this approach. In this stage, entities with insufficient fitness are excluded from the circle, causing rapid convergence. BWOA can inspect a vast region to find the optimum global solution, providing stellar performance in the exploitation and exploration processes; this gives the ability to avoid local optima difficulties and quick convergence speed. This BWOA begins with a search agent (population) of spiders, with each spider denoting a viable candidate. These first spiders endeavor to spawn a new generation as couples. The movement and pheromone are the key elements of the proposed BWOA.

The mathematical modeling of the BWOA is described as follows:

Movement: as indicated in Equation (7), the spider's moves inside the web were characterized as linear and spiral.

$$\vec{p}_i(n+1) = \begin{cases} \vec{p}_{best}(n) - q\vec{p}_{r_1}(n) & if\ rand() \leq 0.3 \\ \vec{p}_{best}(n) - \cos(2\pi\delta)\vec{p}_i(n) & for\ other\ circumstance \end{cases} \tag{7}$$

where, $\vec{p}_i(n+1)$ is the new position of a search agent, $\vec{p}_{best}(n)$ is the previous iteration best search agent, $q$ represents the randomly generated float number between [0.4, 0.9], $r_1$ varies between 1 and the maximum size of search agents generated by a random integer number, $\vec{p}_{r_1}(n)$- position of the $r_1$ search agent, with $i \neq r_1$, $\delta$ is the randomly generated float number in the interval $[-1.0, 1.0]$, $\vec{p}_i(n)$ is the position of the current search agent.

Pheromones: pheromone is a significant phenomenon in the mating of spiders. A female spider with low pheromone rates indicates a hungry cannibal spider. Male spiders typically do not prefer female spiders with low pheromone rates. For low pheromone rates, scores of 0.3 or below, it would be substituted by another female spider. Based on Equation (8), the spider updates its position and moves towards an option to avoid the female spiders with low pheromone rates. The equation represents the pheromone rate value.

$$pheromone\ (i) = \frac{(fitness_{worst} - fitness(i))}{(fitness_{worst} - fitness_{best})} \tag{8}$$

where, $fitness_{worst}$ is the current generation worst fitness value, $fitness_{best}$ is the current generation best fitness value, $fitness(i)$ is the $i$th search agent's current fitness value.

Updating of search agent:

$$\vec{p}_i(n) = \vec{p}_{best}(n) + \frac{1}{2}\left[\vec{p}_{r_1}(n) - (-1)^\gamma * \vec{p}_{r_2}(n)\right] \tag{9}$$

where $\vec{p}_i(n)$ is the low pheromone rate search agent is going to be modified, $r_1$ and $r_2$ are random integer numbers derived between 1 and the maximum size of search agents, provided $r_1 \neq r_2$, $\vec{p}_{r_1}(n)$, $\vec{p}_{r_2}(n)$- $r_1, r_2$ chosen search agents, $\vec{p}_{best}(n)$ is best past iterations best search agent, $\gamma$ is a randomly generated binary number, $\gamma \in \{0, 1\}$.

The proposed algorithm updates the low pheromone rate search agent instead of the whole search agent updating before the next iteration, enhancing the fitness quality and leading to better equilibrium between the exploitation and exploration processes.

Strengths of the BWOA:

- Easy to implement;
- Better convergence speed;

- Significantly avoids the entrapment of local optima;
- Satisfactory accuracy;
- Reduced complexity.

Weakness of the BWOA: BWOA belongs to the metaheuristic algorithm; hence it cannot ensure that it will discover the best result.

Procedures of the black widow optimization algorithm:

The following procedures are incurred in the proposed BWOA.

*Procedure 1*: start

*Procedure 2:* perform the initialization of variable and search agents

*Procedure 3:* carry out the computation of the spider movements using Equation (6), for each iteration, the $q$ and $\delta$ varies between the range $-1.0 \leq \delta \leq 1.0$ and $0.4 \leq q \leq 0.9$ randomly. The value of $q$ and $\delta$ responsible for the linear and spiral movement, respectively.

*Procedure 4:* using Equation (7), calculate each search agent's pheromone rate.

*Procedure 5:* using Equation (8), update the search agent.

*Procedure 6:* compute the new fitness value ($\vec{p}_{new}(n)$) new search agent. If $\vec{p}_{new}(n) < \vec{p}_{best}(n)$ then $\vec{p}_{new}(n) = \vec{p}_{best}(n)$.

*Procedure 7:* increment the iteration (i.e., Iteration = iteration +1).

*Procedure 8:* record the best optimal value $\vec{p}_{best}(n)$.

*Procedure 9*: terminate.

The flowchart of the proposed algorithm based on solar cell/panel parameter extraction is shown in Figure 2. The PV cell/panels parameters extraction is considered as the single objective optimization problem with the objective function of minimization of error (RMSE). The proposed BWOA set parameters are dimension: 5 (SDM) and 7 (DDM), number of search agents (populations): 250, and number of iterations: 1500.
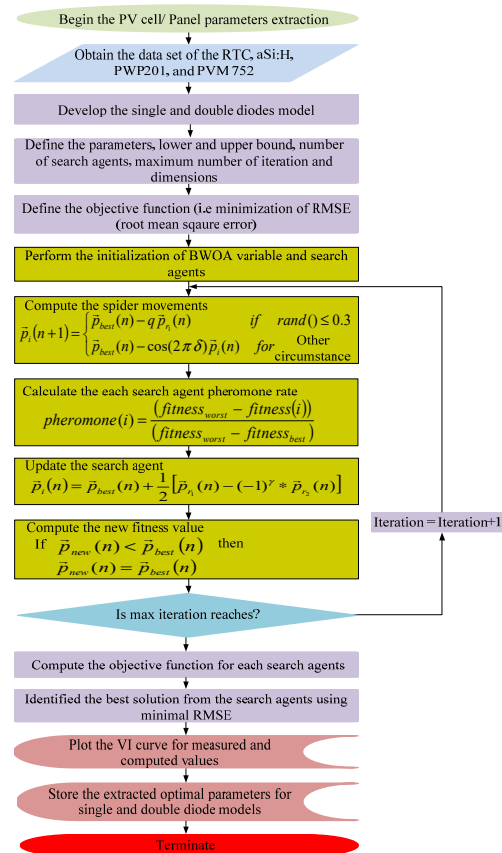


**Figure 2.** Flow chart of PV cell/panel parameter extraction using the BWOA.

### 3. Results and Discussions

Four photovoltaic devices, two photovoltaic cells RTC France and amorphous silicon, and two photovoltaic panels PWP201 and PVM 752 GaAs are considered to verify the performance of the BWOA. The comparison with the algorithms is made by analyzing the results for root mean square error, mean relative error, mean bias error, the coefficient of determination, and adjusted coefficient of determination. First, the algorithm was applied to extract the parameters using 1500 iterations and 250 populations.

The current-voltage characteristic from RTC silicon photovoltaic cell is measured at 1000 W/m$^2$ and 33 °C temperature. The dataset [35], the values for current calculated using the BWOA for both models SDM and DDM, and the errors are presented in Table S1. The extracted parameters for both models SDM and DDM using the BWOA are presented in Table 2, where $I_{ph}$ is the photogenerated current, $I_0$ is the reverse saturation current, n represents the ideality factor of the diode, $R_s$ is series resistance, and $R_{sh}$ is shunt resistance.

**Table 2.** The parameters of RTC photovoltaic cell.

| Model | $I_{ph}$ [A] | $I_{o1}$ [μA] | $n_1$ | $R_s$ [Ω] | $R_{sh}$ [Ω] | $I_{o2}$ [μA] | $n_2$ |
|---|---|---|---|---|---|---|---|
| SDM | 0.760775530434 | 0.323020844639 | 1.48118360077909 | 0.03637709229298 | 53.71852777362 | - | - |
| DDM | 0.760788874901 | 0.231811940424 | 1.45130774253217 | 0.03686252219760 | 56.97316671933 | 2.843617195413 | 2.4133546221726 |

The results for the five statistical tests obtained using the extracted parameter from the BWOA and the best metaheuristic algorithms are given in Table 3. It can be observed that BWOA gives the best results for all statistical tests, for both analysis models. MRE and MBE have the best improvements. The adjusted coefficient of determination shows that all five parameters are significant. Whereas the RMSE value given by the considered algorithms is very good for the SDM model, it becomes less good for the DDM models, apart from the HSDA algorithm. The genetic algorithm and particle swarm optimization have poor results for RMSE. The problem with the genetic algorithm is that it falls within the local minimum. The algorithms from the particle swarm optimization (PSO) family have some advantages in comparison with the genetic algorithm, but the results can be improved. The RMSE for the genetic algorithm is 0.01908 and for PSO it is 0.001386 in the case of the SDM model. Using hybridization, the performance of both algorithms is improved. The genetic algorithm with convex combination crossover has better RMSE for both models in comparison with the niche particle swarm optimization in parallel computing, and the RMSE of both algorithms are very close to the ones given by BWOA. RMSE obtained using the black widow optimization algorithm version is poor. RMSE is 0.0026 for pheromone value BWOA and 0.0071 for cannibalism BWOA in the case of the SDM model, and 0.0033 and 0.0075, in the case of the DDM model, respectively [31].

**Table 3.** Statistical tests of the RTC photovoltaic cell for different algorithms.

| Algorithms | Model | RMSE | MRE | MBE | $R^2$ | $R_a^2$ | Computing Time [s] |
|---|---|---|---|---|---|---|---|
| **BWOA** | **SDM** | **0.00098602187** | **0.00150107** | **$9.6050008 \times 10^{-11}$** | **0.999989306** | **0.999986632** | **1.965546** |
| HDSA | SDM | 0.00098602189 | 0.00739214 | $1.42971 \times 10^{-8}$ | 0.999989306 | 0.999986632 | 22.12423 |
| ISCE | SDM | 0.00098602189 | 0.0074567 | $-8.61057 \times 10^{-9}$ | 0.9999893 | 0.999986625 | - |
| IWOA | SDM | 0.000986022 | 0.00645125 | $6.71469 \times 10^{-5}$ | 0.99998911 | 0.999986388 | - |
| ILCOA | SDM | 0.000986022 | 0.0081267 | $2.2791 \times 10^{-7}$ | 0.99998923 | 0.999986537 | - |

**Table 3.** *Cont.*

| Algorithms | Model | RMSE | MRE | MBE | $R^2$ | $R_a{}^2$ | Computing Time [s] |
|---|---|---|---|---|---|---|---|
| MLBSA | SDM | 0.000986022 | 0.0081209 | $2.3011 \times 10^{-7}$ | 0.99998923 | 0.999986537 | 44.1 |
| ImSMA | SDM | 0.001166644 | 0.124608 | $-6.44794 \times 10^{-2}$ | 0.99978923 | 0.999986537 | - |
| GACCC | SDM | 0.0009860298 | 0.0073618 | $2.14019 \times 10^{-6}$ | 0.999989306 | 0.999986632 | - |
| NPSOPC | SDM | 0.00098856 | 0.005509 | $9.414449 \times 10^{-5}$ | 0.99997123 | 0.999964037 | - |
| EJADE | SDM | 0.000986022 | 0.00739214 | $1.42971 \times 10^{-8}$ | 0.999989306 | 0.999986632 | 11.82 |
| **BWOA** | **DDM** | **0.0009773823** | **0.00761577** | $\mathbf{2.61366 \times 10^{-8}}$ | **0.999989493** | **0.999985407** | **2.166910** |
| HDSA | DDM | 0.000982174 | 0.00801231 | $-3.30237 \times 10^{-6}$ | 0.99998939 | 0.999985264 | 24.21267 |
| ISCE | DDM | 0.000982485 | 0.00800123 | $-9.32695 \times 10^{-10}$ | 0.99998938 | 0.99998525 | - |
| IWOA | DDM | 0.00098255 | 0.00832156 | $2.03269 \times 10^{-8}$ | 0.99998939 | 0.999985264 | - |
| ILCOA | DDM | 0.00098257 | 0.00832123 | $-4.5227 \times 10^{-7}$ | 0.99998939 | 0.999985264 | - |
| MLBSA | DDM | 0.00098249 | 0.00801432 | $1.03269 \times 10^{-9}$ | 0.99998938 | 0.99998525 | 39.2 |
| GACCC | DDM | 0.00098249 | 0.00775781 | $1.49564 \times 10^{-6}$ | 0.999989382 | 0.999985253 | - |
| NPSOPC | DDM | 0.00098294 | 0.00773652 | $6.02285 \times 10^{-6}$ | 0.999989372 | 0.999985239 | - |
| EJADE | DDM | 0.00098363 | 0.00783214 | $5.41871 \times 10^{-6}$ | 0.999989388 | 0.999985243 | 23.16 |

The best results are highlighted in bold.

The current-voltage characteristic for the silicon amorphous photovoltaic cell is measured at 1000 W/m$^2$ irradiance and 25 °C temperature. The calculated values for the current of the aSi photovoltaic cell, the data set [9], and the errors are presented in Table S2.

The five and seven extracted parameters for both models SDM and DDM of the aSi photovoltaic cell using the BWOA are presented in Table 4.

**Table 4.** The parameters of aSi photovoltaic cell.

| Model | $I_{ph}$ [A] | $I_{o1}$ [µA] | $n_1$ | $R_s$ [Ω] | $R_{sh}$ [Ω] | $I_{o2}$ [µA] | $n_2$ |
|---|---|---|---|---|---|---|---|
| SDM | 0.011344722027 | 0.734937259184 | 3.3684179763920 | 0.01 | 523.1534162533 | - | - |
| DDM | 0.011343901356 | 3.499752108404 | 4.9992795225461 | 0.3800093610916 | 554.6414716819 | 0.156114790404 | 2.9571967602922 |

The results for the five statistical tests obtained using the extracted parameters from the BWOA and the best metaheuristic algorithms are given in Table 5. There are very few algorithms that are currently applied to extract the parameters of aSi photovoltaic cell. The BMOA is used instead of IWOA algorithm for the biology group. The five-parameters method is also used to extract parameters for the SDM model [4]. BWOA is by far the best, especially for the DDM model. RMSE obtained using HSDA is very close for the SDM model. The computational time for BWOA is two times lower than the following algorithm.

**Table 5.** Statistical tests of the aSi photovoltaic cell for different algorithms.

| Algorithms | Model | RMSE | MRE | MBE | $R^2$ | $R_a{}^2$ | Computing Time [s] |
|---|---|---|---|---|---|---|---|
| **BWOA** | **SDM** | $\mathbf{4.6123219 \times 10^{-5}}$ | **0.004161571** | $\mathbf{2.159066442 \times 10^{-12}}$ | **0.9999702** | **0.999966475** | **2.094126** |
| HDSA | SDM | $4.619456 \times 10^{-5}$ | 0.0042345 | $4.13577 \times 10^{-7}$ | 0.999665 | 0.999623125 | 18.1212 |
| BMOA | SDM | $8.2115 \times 10^{-5}$ | 0.0073431 | $-1.6201 \times 10^{-6}$ | 0.997365 | 0.997035625 | 4.746904 |

**Table 5.** *Cont.*

| Algorithms | Model | RMSE | MRE | MBE | $R^2$ | $R_a^2$ | Computing Time [s] |
|---|---|---|---|---|---|---|---|
| 5P | SDM | $2.08631\ 4 \times 10^{-4}$ | 0.0153567 | $-0.000144047$ | 0.993170 | 0.99231625 | - |
| **BWOA** | **DDM** | $\mathbf{4.2586126 \times 10^{-5}}$ | **0.0037876085** | $\mathbf{-9.393959725 \times 10^{-9}}$ | **0.999977** | **0.999972763** | **2.338393** |
| HDSA | DDM | $4.4973518 \times 10^{-5}$ | 0.00801231 | $2.63015 \times 10^{-8}$ | 0.999683 | 0.999624605 | 19.23451 |
| BMOA | DDM | $5.3511 \times 10^{-5}$ | 0.0046531 | $3.7606 \times 10^{-7}$ | 0.999467 | 0.999368816 | 5.520116 |

Best results are highlighted in bold.

The PWP201 photovoltaic panel has 36 polycrystalline silicon photovoltaic cells. These cells are connected in series. The current-voltage characteristic for the PWP201 photovoltaic panel is measured at 1000 W/m$^2$ irradiance and 45 °C temperature [35]. The calculated values for the current of the PWP201 photovoltaic panel using the BWOA for both models SDM and DDM, the data set, and the errors are presented in Table S3.

The extracted parameters of the PWP201 photovoltaic panel in both cases using the BWOA are shown in Table 6.

**Table 6.** The parameters of the PWP201 photovoltaic panel.

| Model | $I_{ph}$ [A] | $I_{o1}$ [µA] | $n_1$ | $R_s$ [Ω] | $R_{sh}$ [Ω] | $I_{o2}$ [µA] | $n_2$ |
|---|---|---|---|---|---|---|---|
| SDM | 1.030514298911 | 3.482262763248 | 48.6428346965937 | 1.20127101509370 | 981.9822671055 | - | - |
| DDM | 1.030467877304 | 0.509349656031 | 49.7918122619372 | 1.20084582205427 | 990.1811809837 | 3.007105049127 | 48.523613004943 |

The results for the five statistical tests obtained using the extracted parameter from the BWOA and the best metaheuristic algorithms are presented in Table 7. The dataset of PWP201 photovoltaic panel is the most used after the one for the RTC cell. RMSE, $R^2$, $R_a^2$ for the SDM model are almost equal for BWOA, HSDA, ISCE, MLBSA, GACCC, NPSOPC, and EJADE. The BWOA has better results for MRE and MBE. BWOA shows its superiority for the five statistical tests for the DDM model. The computing time is the smallest one. The RMSE obtained using the black widow optimization algorithm versions is poor. The RMSE is 0.0035 for pheromone value BWOA and 0.0059 for cannibalism BWOA in the case of the SDM model, and 0.005 and 0.0051, respectively, in the case of the DDM model [31].

**Table 7.** Statistical tests of the PWP201 photovoltaic panel for different algorithms.

| Algorithms | Model | RMSE | MRE | MBE | $R^2$ | $R_a^2$ | Computing Time [s] |
|---|---|---|---|---|---|---|---|
| **BWOA** | **SDM** | **0.0024250748** | **0.003048773** | $\mathbf{1.670003 \times 10^{-10}}$ | **0.999970116** | **0.999962252** | **2.003670** |
| HDSA | SDM | 0.0024250748 | 0.00599652 | $-9.49346 \times 10^{-10}$ | 0.999970116 | 0.999962252 | 21.32178 |
| ISCE | SDM | 0.002425075 | 0.00599652 | $-9.49475 \times 10^{-9}$ | 0.999970116 | 0.999962252 | - |
| EHHO | SDM | 0.00242508 | 0.00599744 | $-9.43245 \times 10^{-9}$ | 0.999970116 | 0.999962252 | - |
| IWOA | SDM | 0.0024251 | 0.00846125 | $5.21469 \times 10^{-5}$ | 0.999970511 | 0.999962751 | - |
| ER-WCA | SDM | 0.0024378989 | 0.00511445 | $1.23842 \times 10^{-4}$ | 0.999969799 | 0.999961851 | - |
| MLBSA | SDM | 0.002425075 | 0.00612177 | $1.83197 \times 10^{-5}$ | 0.999970115 | 0.999962251 | 43.44 |
| GACCC | SDM | 0.0024250748 | 0.00599767 | $2.52888 \times 10^{-7}$ | 0.999970116 | 0.999962252 | - |
| NPSOPC | SDM | 0.0024250762 | 0.00601738 | $1.61452 \times 10^{-6}$ | 0.999970116 | 0.999962252 | - |
| EJADE | SDM | 0.0024251 | 0.00846125 | $5.40469 \times 10^{-5}$ | 0.999970511 | 0.999962751 | 11.85 |

**Table 7.** *Cont.*

| Algorithms | Model | RMSE | MRE | MBE | $R^2$ | $R_a{}^2$ | Computing Time [s] |
|---|---|---|---|---|---|---|---|
| **BWOA** | **DDM** | **0.0024260068** | **0.003052412** | **$5.1019716 \times 10^{-6}$** | **0.999970091** | **0.999957776** | **2.163120** |
| HDSA | DDM | 0.002587754 | 0.0107405 | $-5.3062 \times 10^{-5}$ | 0.999965972 | 0.99995196 | 22.32145 |
| BMOA | DDM | 0.0041767 | 0.0056796 | $5.3913 \times 10^{-4}$ | 0.999923401 | 0.99989186 | 7.59144 |
| GCPSO | DDM | 0.0026313 | 0.0137405 | $-3.64427 \times 10^{-5}$ | 0.999965991 | 0.99995198 | - |

The best results are highlighted in bold.

The dataset of the PVM 752 GaAs thin-film photovoltaic panel is measured at the national renewable energy laboratory (NREL) [36], the values obtained using the BWOA for both models SDM and DDM, and the errors are presented in Table S4. The current-voltage characteristic for PVM 752 GaAs thin-film photovoltaic panel is measured at 1000 W/m$^2$ irradiance and 25 °C temperature.

The extracted five and seven parameters of the PVM 752 GaAs photovoltaic panel using the BWOA are given in Table 8.

**Table 8.** The parameters of PVM 752 GaAs thin-film photovoltaic panel.

| Model | $I_{ph}$ [A] | $I_{o1}$ [μA] | $n_1$ | $R_s$ [Ω] | $R_{sh}$ [Ω] | $I_{o2}$ [μA] | $n_2$ |
|---|---|---|---|---|---|---|---|
| SDM | 0.100066825796 | $3.7788963 \times 10^{-12}$ | 1.6156728332454 | 0.6605088752480 | 608.0099343761 | - | - |
| DDM | 0.100010673592 | 9.988550426791 | 7.17885667016653 | 0.67249614174253 | 983.1116498983 | $1.5226865 \times 10^{-12}$ | 1.5577162075783 |

The results for the five statistical tests obtained using the extracted parameter from the BWOA and the best metaheuristic algorithms are given in Table 9. BWOA shows its performance for the PVM 752 GaAs thin-film photovoltaic panel for both SDM and DDM models. RMSE obtained by BWOA is improved (decreasing) by 3% in comparison with HSDA algorithm, which is the second in the case of the SDM model, and with 16.5% in the case of the DDM model. Additionally, the computing time for BWOA is very low, ten times lower than HSDA.

**Table 9.** Statistical tests of PVM 752 GaAs thin-film photovoltaic panel for different algorithms.

| Algorithms | Model | RMSE | MRE | MBE | $R^2$ | $R_a{}^2$ | Computing Time [s] |
|---|---|---|---|---|---|---|---|
| **BWOA** | **SDM** | **0.00022780382** | **0.002452525** | **$3.827646 \times 10^{-12}$** | **0.999960795** | **0.999955636** | **2.054059** |
| HDSA | SDM | 0.0002346967 | 0.00739214 | $4.21357 \times 10^{-9}$ | 0.999960057 | 0.999954801 | 20.23141 |
| EHHO | SDM | 0.0023910170 | 0.0545125 | $5.64302 \times 10^{-6}$ | 0.9961378 | 0.995629616 | - |
| SDO | SDM | 0.0002369980 | 0.0034367 | $3.2839 \times 10^{-5}$ | 0.9999576 | 0.999952021 | - |
| MLBSA | SDM | 0.002384 | 0.621396 | $1.26592 \times 10^{-3}$ | 0.996444355 | 0.995976507 | - |
| **BWOA** | **DDM** | **0.0001778193** | **0.00761577** | **$-1.6920782 \times 10^{-6}$** | **0.999976112** | **0.999971467** | **2.351128** |
| HDSA | DDM | 0.0002130617 | 0.00801231 | $-1.77149 \times 10^{-7}$ | 0.999965734 | 0.999959071 | 21.32567 |
| EHHO | DDM | 0.0022610170 | 0.00832156 | $5.64302 \times 10^{-6}$ | 0.9961378 | 0.995386817 | - |
| SDO | DDM | 0.0002231310 | 0.00345623 | $-6.18891 \times 10^{-5}$ | 0.9999624 | 0.999955089 | - |
| MLBSA | DDM | 0.00352 | 0.7234 | $1.2749 \times 10^{-3}$ | 0.99645635 | 0.995767307 | - |

The best results are highlighted in bold.

Comparing the results obtained using the BWOA for the RMSE, which is the most important statistical test, with the ones obtained using the best algorithms which are in the specialized literature from the four groups considered, the superiority of the BWOA can easily be observed, see Table 10. The best improvements are obtained for the two-diode model. For all four photovoltaic cells and panels, BWOA gives lower results in RMSE. The

decrease is from 0.5% for RTC photovoltaic cell to 16.5% for the PVM 752 GaAs. The same results in RMSE are obtained for the PWP 201 photovoltaic panel and very little lower for the RTC photovoltaic panel when the one-diode model was considered.

**Table 10.** The improvements in RMSE.

| Photovoltaic Cell or Panel | Model | Gain |
|---|---|---|
| RTC | SDM | 0% |
| | DDM | 0.5% |
| aSi | SDM | 0.5% |
| | DDM | 5.3% |
| PWP 201 | SDM | 0% |
| | DDM | 6.25% |
| PVM 752 GaAs | SDM | 3% |
| | DDM | 16.5% |

All the above results for the RTC photovoltaic cell, aSi photovoltaic cell, PWP 201 photovoltaic panel, and PVM 752 GaAs photovoltaic panel are obtained using 1500 iterations and 250 population numbers. The number of iterations and the population were varied to optimize the extraction process as a value of RMSE and computing time. Table S5a–d presents all the results for both models, two numbers of iterations, and several numbers of populations.

A short computing time to extract the parameters is very important for manufacturers in the production process. Taking into consideration this target, the population number was varied from 15 to 250 (from 50 to 250 with step by 25) for two iterations numbers 500 and 1500. The convergence speed depends on the size of the population. A small population leads to faster convergence but increases the possibility of falling into a local minimum, while a large population can improve the exploration ability and avoid falling into a local minimum, but the convergence speed decreases.

The population under 100 gives low results in RMSE, which shows that the algorithm finds the local minimum, rather than the global one. The computing time is shorter, but this seriously affects the performance of the algorithm.

When the SDM model is used, a good performance is obtained for a small population rather than for the DDM model, but there is no model. For example, for the PWP201 photovoltaic panel, the best results are obtained for 175 populations in the SDM case and 125, respectively, for the DDM model. Unfortunately, the computing time is not lower if the population number is smaller than 250, and the results in RMSE are very good. Still, analyzing the results, the computing time can be reduced by more than 30% with a very small increase in RMSE, which can be accepted for the manufacturing process.

The computing time for extracting the parameters with BWOA is far lower than for the other algorithms, around 2 s. Still, it depends on the computer's specifications to run the algorithm. The features of the computers used are the following: BWOA runs on Intel Core 9, 10 Core (s), 3.6 GHz 20 MB; GPU: NVIDIA GeForce RTX 3080Ti 12 GB; RAM: 32 GB; HDSA runs on Intel Core 7, 8-thread, 1.9 GHz; MLBSA run on PC Intel Core 3 Duo 3.30 GHz with a 4 GB RAM that runs on Windows 10 with MATLAB R2022a implementation.

By analyzing the results presented in Table S5, the best results for RMSE are included in Table 11 for all four photovoltaic devices. The best results are obtained for 1500 iterations, but not for the maximum population number 250. For the RTC photovoltaic cell the best results are obtained using 175 populations in the case of the SDM model and 250 for the DDM model. For aSi if 200 population is used for the SDM model and 225 population for the DDM model, for the last cases, a very good improvement is observed, with RMSE being lower by almost 4%. The best results are obtained for the PWP 201, if a 175 population is used for the SDM model and a 125 population for the DDM model. The best results

are obtained for PVM 752 GaAs, if a 250 population is used for the SDM model and a 225 population for the DDM model.

**Table 11.** The RMSE and computing time function of the iterations and population number.

| Photovoltaic Cell or Panel | Model | Search Agents | Iterations | RMSE | Computing Time [s] |
|---|---|---|---|---|---|
| RTC | SDM | 250 | 500 | 0.00098756008969 | 1.635081 |
| | | 175 | 1500 | **0.0009860218778915** | 2.889780 |
| | DDM | 125 | 500 | 0.00110769738637 | 1.582938 |
| | | 250 | 1500 | **0.000977382318798** | 2.166910 |
| aSi | SDM | 200 | 500 | 0.00004612322475 | 1.687007 |
| | | 200 | 1500 | **0.00004612321932** | 1.959808 |
| | DDM | 225 | 500 | 0.00004346987976 | 1.607626 |
| | | 225 | 1500 | **0.0000409439377149** | 2.749709 |
| PWP 201 | SDM | 250 | 500 | 0.0024250748682 | 1.616498 |
| | | 175 | 1500 | **0.002425074868095** | 2.300761 |
| | DDM | 250 | 500 | 0.0024393543586 | 1.735792 |
| | | 125 | 1500 | **0.0024250748681** | 1.992434 |
| PVM 752 GaAs | SDM | 175 | 500 | 0.00023029317714 | 1.647252 |
| | | 250 | 1500 | **0.000227803829** | 2.054059 |
| | DDM | 100 | 500 | 0.00017114543330 | 1.496219 |
| | | 225 | 1500 | **0.0001677947841902** | 2.284357 |

The best results are highlighted in bold.

The matching between the current-voltage pairs from data sets and those calculated using the BWOA is very good, this being proven by the high value of the coefficient of determination and adjusted coefficient of determination. This can be seen for the RTC photovoltaic cell in Figure 3 for the SDM model and in Figure 4 for the DDM model, and for both models, the coefficient of determination is over 0.999989, and the adjusted coefficient of determination is over 0.999985. Additionally, the individual absolute current error proves that the calculated values for the current for the entire range of voltage measured present a high coincidence with the ones measured. The individual absolute current error varies for the SDM model between $8.77037 \times 10^{-5}$ and 0.002507413. For the DDM model, the minimum is $9.20751 \times 10^{-5}$ and the maximum for the individual absolute current error is 0.002555849.

The aSi photovoltaic cell current-voltage characteristics, measured and calculated, are presented in Figure 5 for the SDM model and in Figure 6 for the DDM model. The matching between the characteristics is very good. This is proven by the high values, for both models, of the coefficient of determination, which is over 0.99997, and the adjusted coefficient of determination, which is over 0.999966. Additionally, the individual absolute current error proves that the calculated values for the current for the entire range of voltage measured present a high coincidence with the ones measured. The individual absolute current error varies for the SDM model between $5.373148 \times 10^{-7}$ and $9.221552 \times 10^{-5}$, and for the DDM model it varies between $3.361195 \times 10^{-6}$ and $9.25594 \times 10^{-5}$.
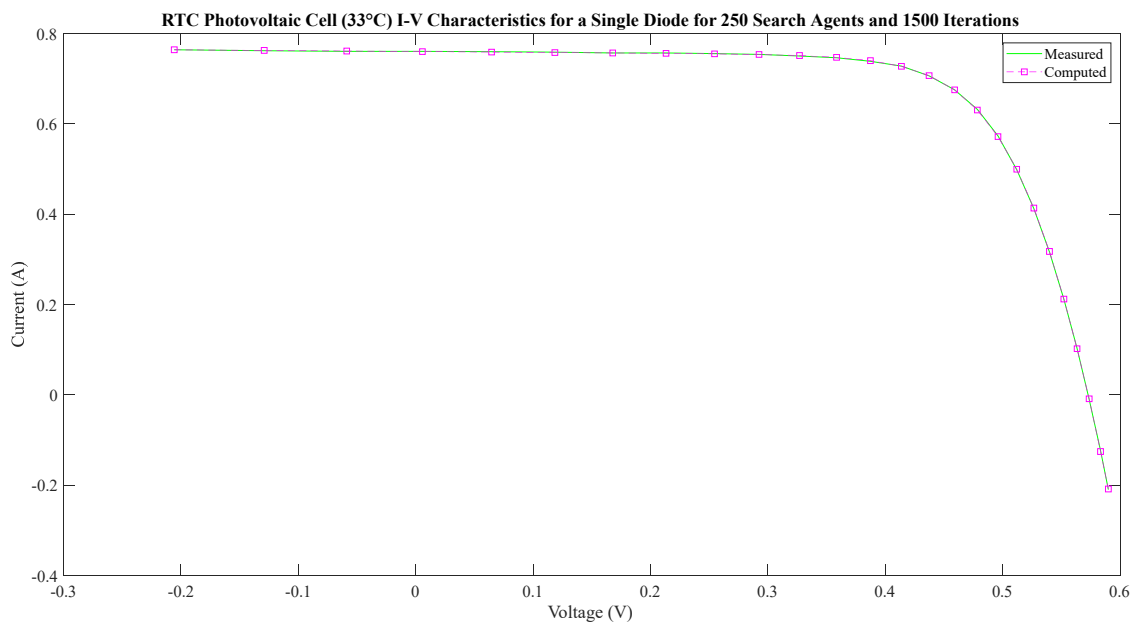
**Figure 3.** The current-voltage characteristics of RTC silicon photovoltaic cell (SDM).
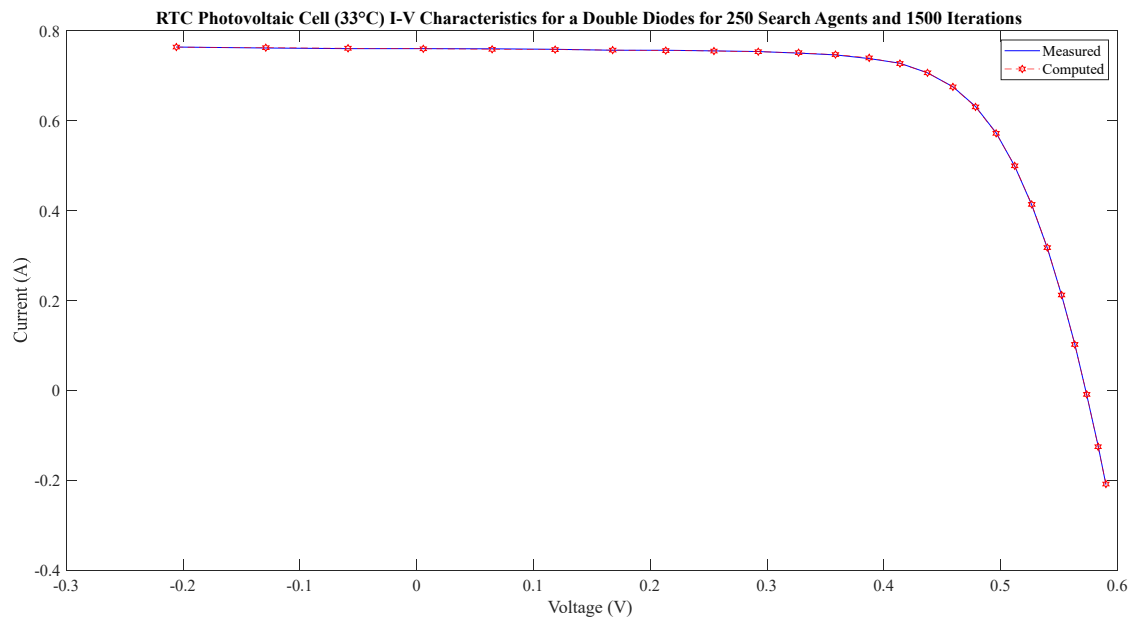


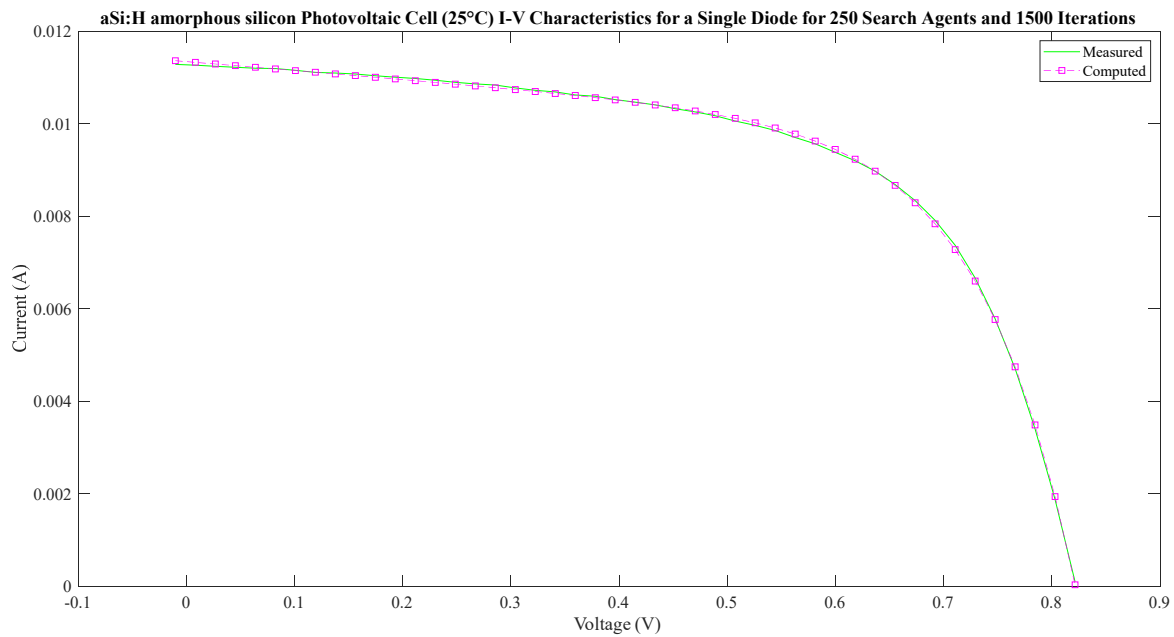**Figure 4.** The current-voltage characteristics of RTC silicon photovoltaic cell (DDM).

**Figure 5.** The current-voltage characteristics of amorphous silicon photovoltaic cell (SDM).
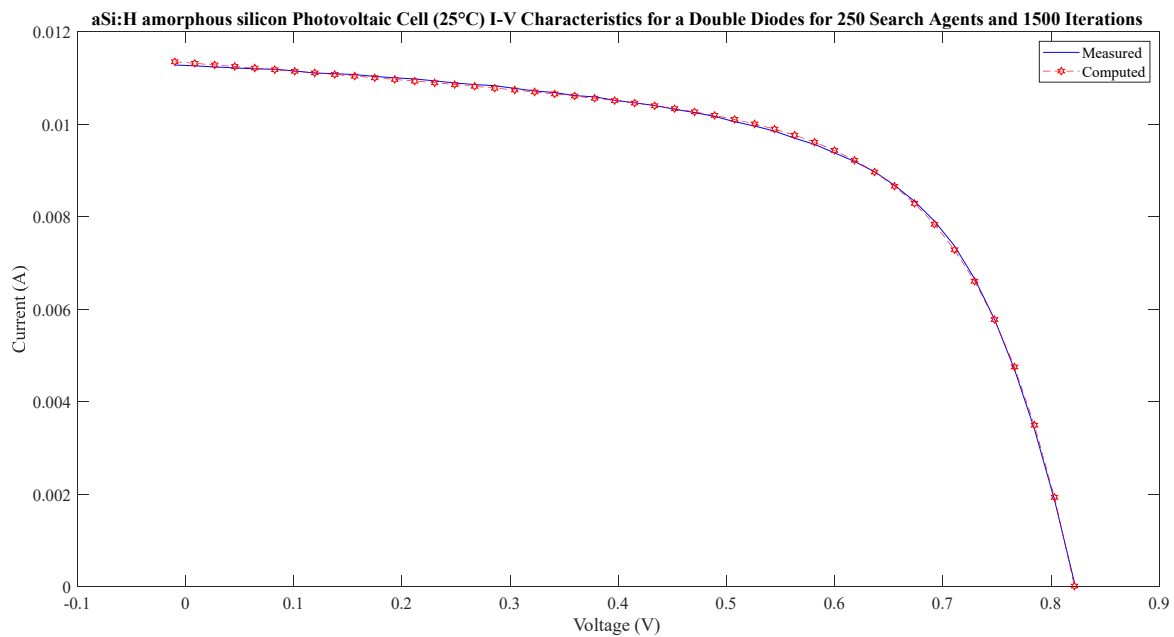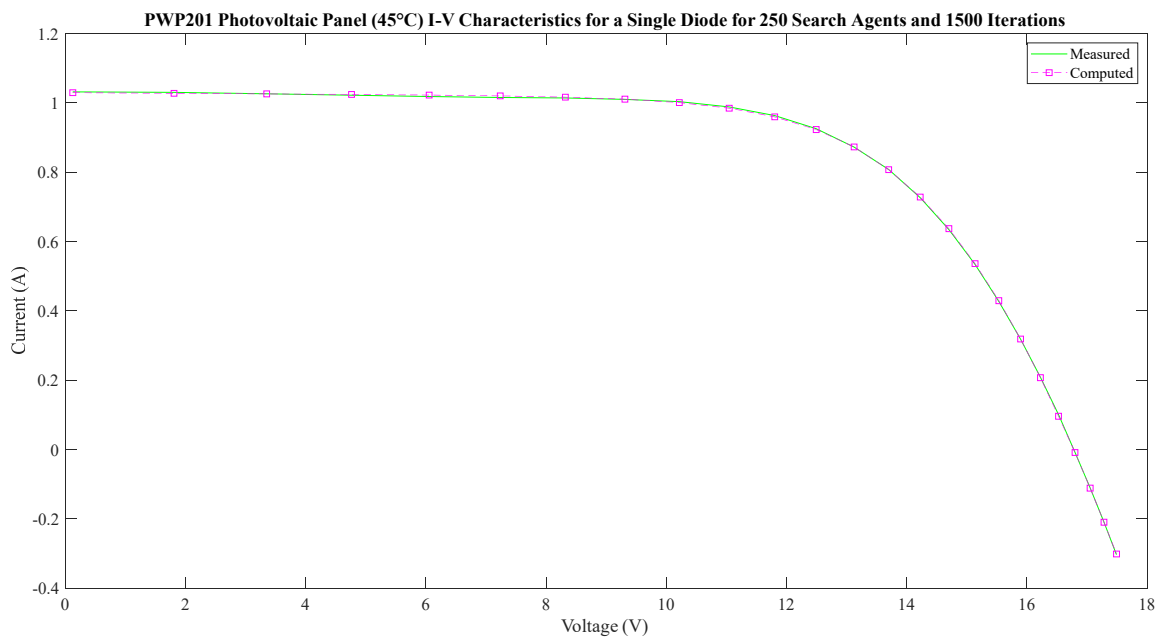


**Figure 6.** The current-voltage characteristics of amorphous silicon photovoltaic cell (DDM).

PWP 201 photovoltaic panel current-voltage characteristics, measured and calculated, are presented in Figure 7 for the SDM model and in Figure 8 for the DDM model. The matching between the characteristics is very good. This is proven by the high values, for both models, of the coefficient of determination over 0.99996, and the adjusted coefficient of determination over 0.999957. Additionally, the individual absolute current error proves that the calculated values for the current for the entire range of voltage measured greatly coincide with the ones measured. The individual absolute current error varies for the SDM model between $6.35175 \times 10^{-5}$ and 0.004832828. For the DDM model, the minimum is $7.6442 \times 10^{-5}$ and the maximum for the individual absolute current error is 0.004807512.
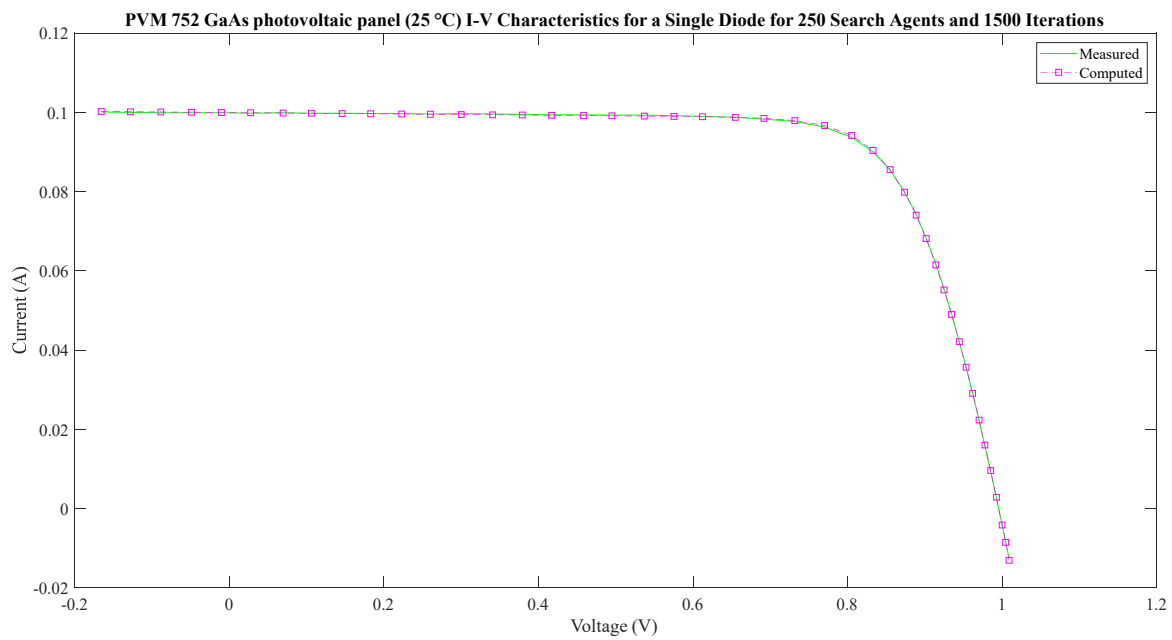
**Figure 7.** The current-voltage characteristics of PWP201 photovoltaic panel for a single diode (SDM).
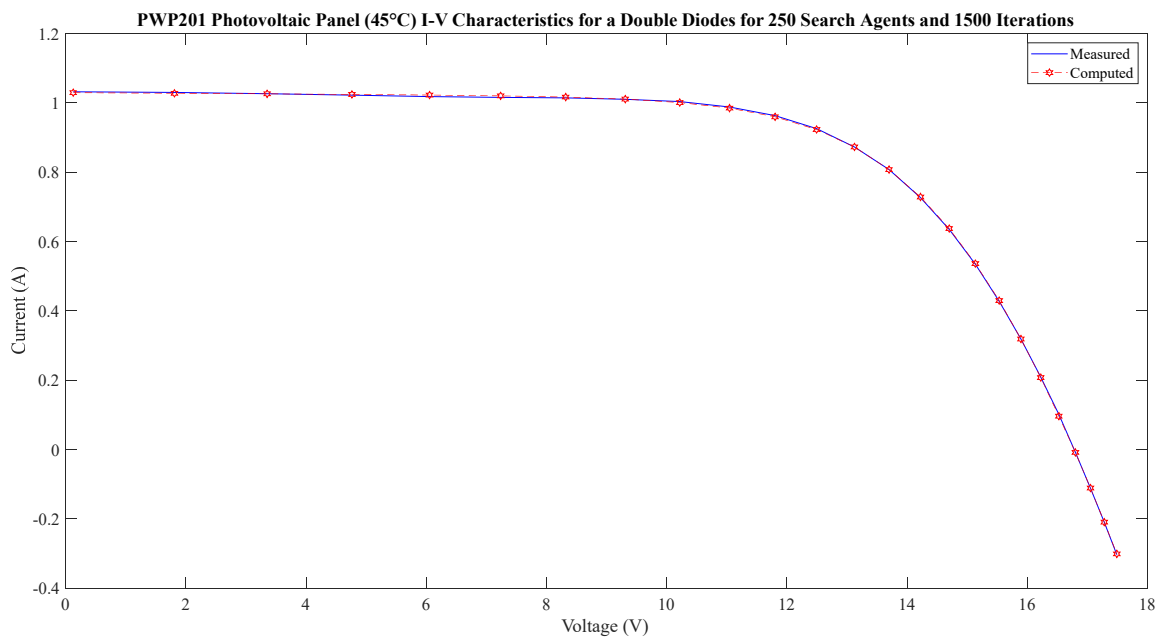


**Figure 8.** The current-voltage characteristics of PWP201 photovoltaic panel for double diodes (DDM).

The PVM 752 GaAs photovoltaic panel current-voltage characteristics, measured and calculated, are presented in Figure 9 for the SDM model and in Figure 10 for the DDM model. The matching between the characteristics is very good. This is proven by the high values, for both models, of the coefficient of determination over 0.99997 and the adjusted coefficient of determination over 0.999955. Additionally, the individual absolute current error proves that the calculated values for the current for the entire range of voltage measured present a high coincidence with the ones measured. The individual absolute current error varies for the SDM model between $1.448386 \times 10^{-7}$ and 0.000472985, and for the DDM model varies between $9.06281 \times 10^{-6}$ and 0.0005496.

**Figure 9.** The current-voltage characteristics of PVM 752 GaAs photovoltaic panel for the single diode (SDM).
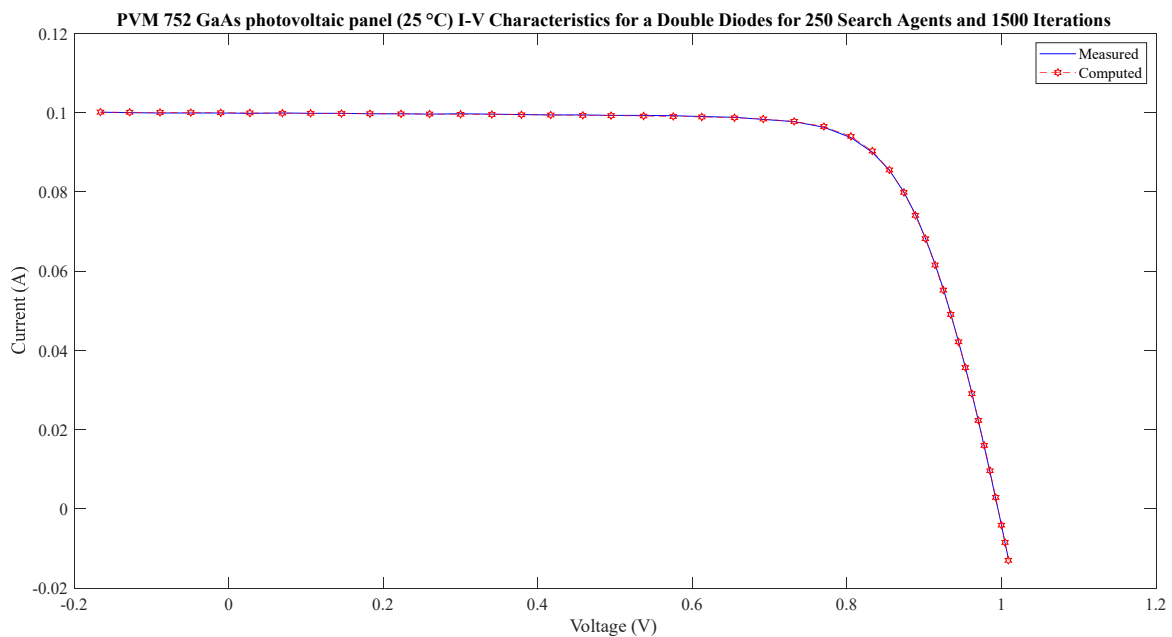


**Figure 10.** The current-voltage characteristics of PVM 752 GaAs photovoltaic panel for double diodes (DDM).

The comparison between the errors in current for the two models shows an alternation, Figure 11 for RTC photovoltaic cell, Figure 12 for aSi photovoltaic cell, Figure 13 PWP 201 photovoltaic panel, and Figure 14 for PVM 752 GaAs photovoltaic panel, there are regions where the errors for SDM are higher than those for DDM, and inversely. Only for the PWP 201 photovoltaic panel, Figure 13, they are almost equal. The ultimate aim of this research work is to extract accurate PV cell and panel parameters with reduced complexity. According to the experimentation results-based analysis, the proposed BWOA is effective, as reduced complexity and computing time also proved the validity with better results to identify the parameters of the photovoltaic cells and panels.
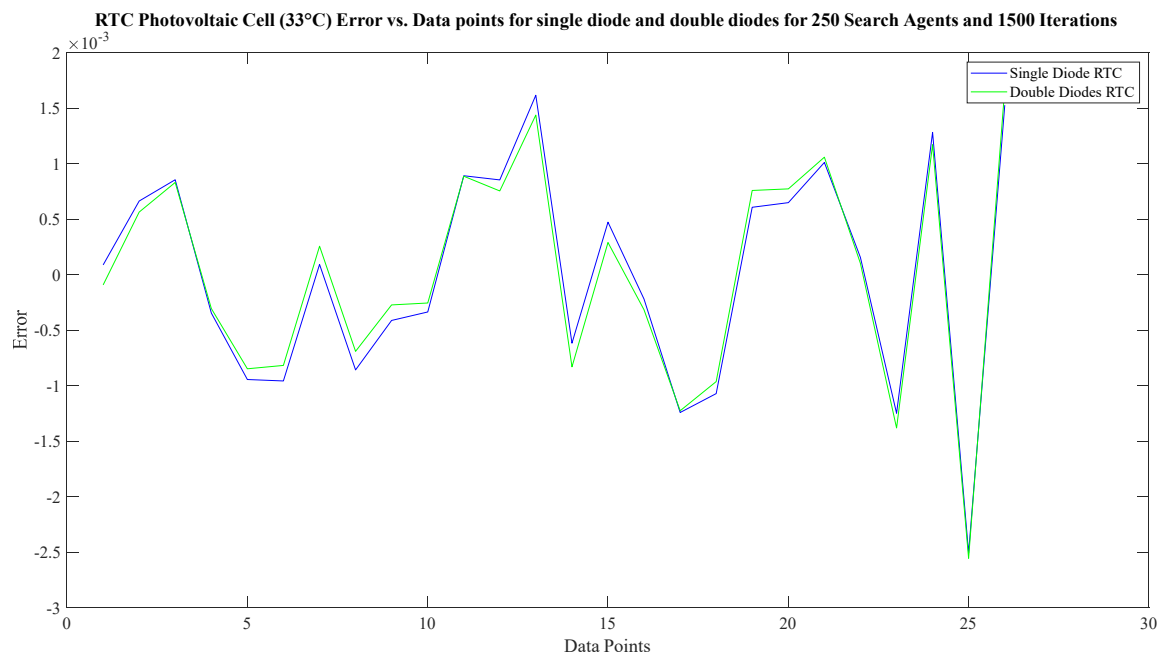
**Figure 11.** Error vs. data points for single diode and double diodes—RTC silicon photovoltaic cell.
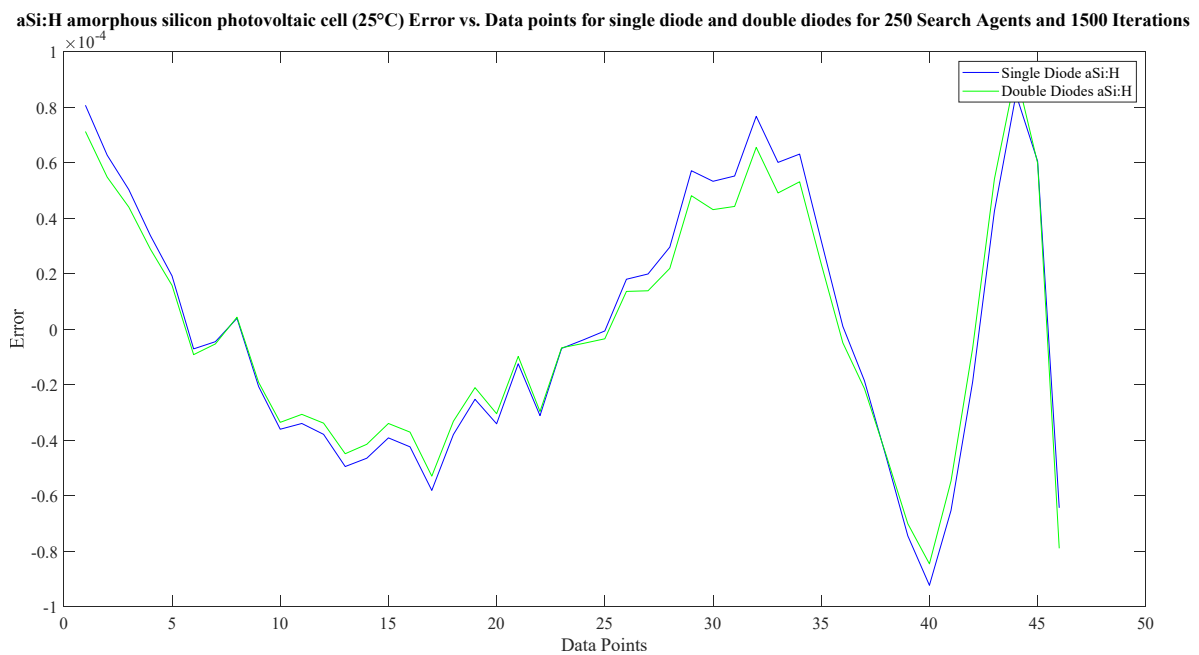


**Figure 12.** Error vs. data points for single diode and double diodes—amorphous silicon photovoltaic cell.
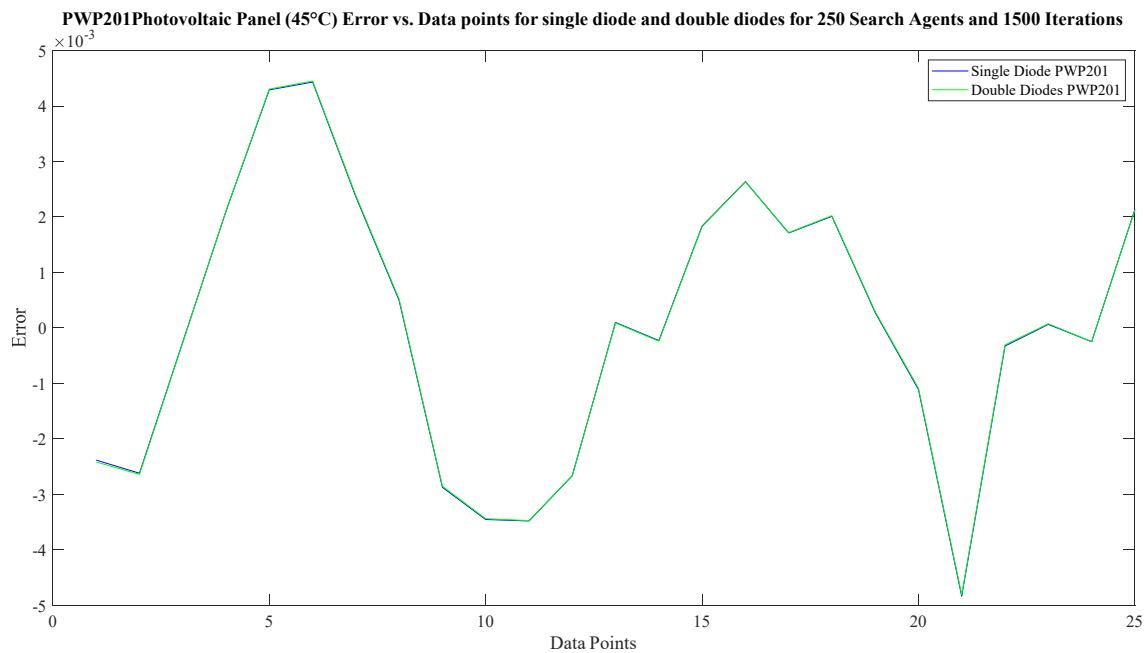
PWP201Photovoltaic Panel (45°C) Error vs. Data points for single diode and double diodes for 250 Search Agents and 1500 Iterations
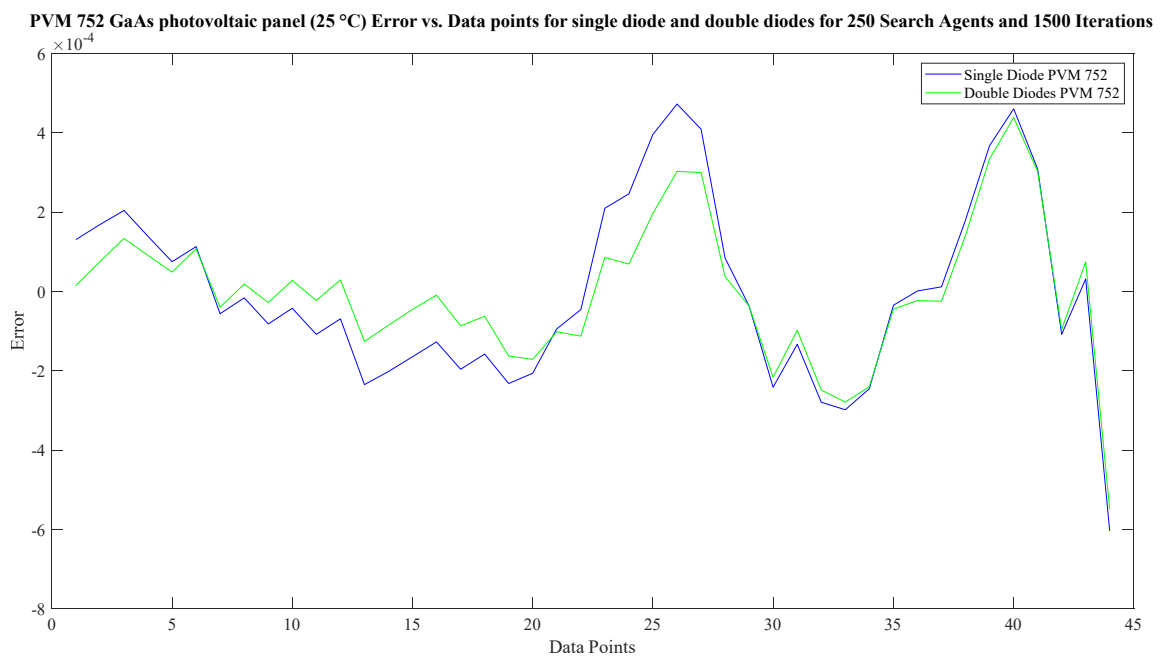


**Figure 13.** Error vs. data points for single diode and double diodes—PWP201 photovoltaic panel.

PVM 752 GaAs photovoltaic panel (25 °C) Error vs. Data points for single diode and double diodes for 250 Search Agents and 1500 Iterations



**Figure 14.** Error vs. data points for single diode and double diodes—PVM 752 GaAs photovoltaic panel.

The proposed BWOA-based PV cell and panels parameters extraction achieved better results with reduced computing time for both SDM and DDM. For a better understanding, Figure 15 illustrates BWOA computing time vs. the number of search agents for the RTC cell, aSi cell, PWP 201 panel, and PVM 752 panel. The ultimate aim of this research work is to extract PV cell and panel parameters accurately and with reduced complexity, computing time, and optimal results. According to the experimentation results-based analysis, the proposed BWOA is effective, presents reduced complexity and the computing time also proved the validity with better results to identify the parameters of the photovoltaic cells and panels.
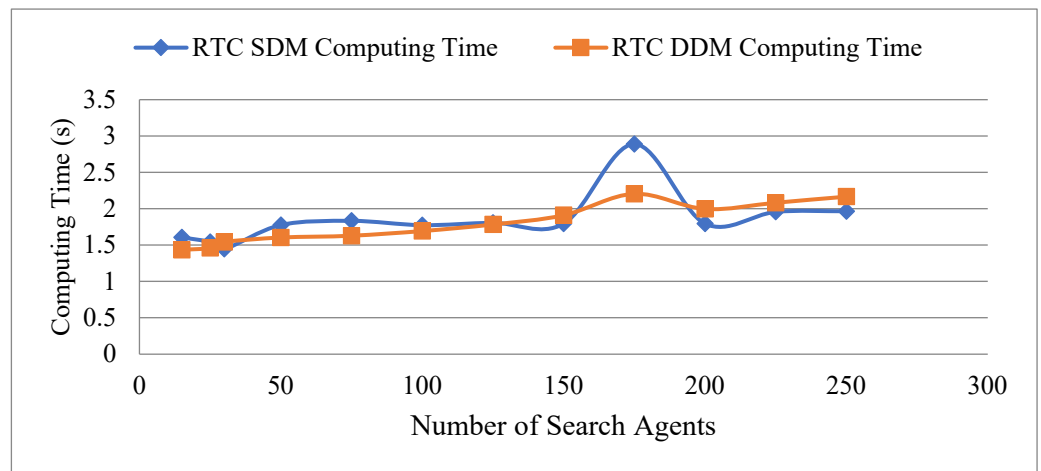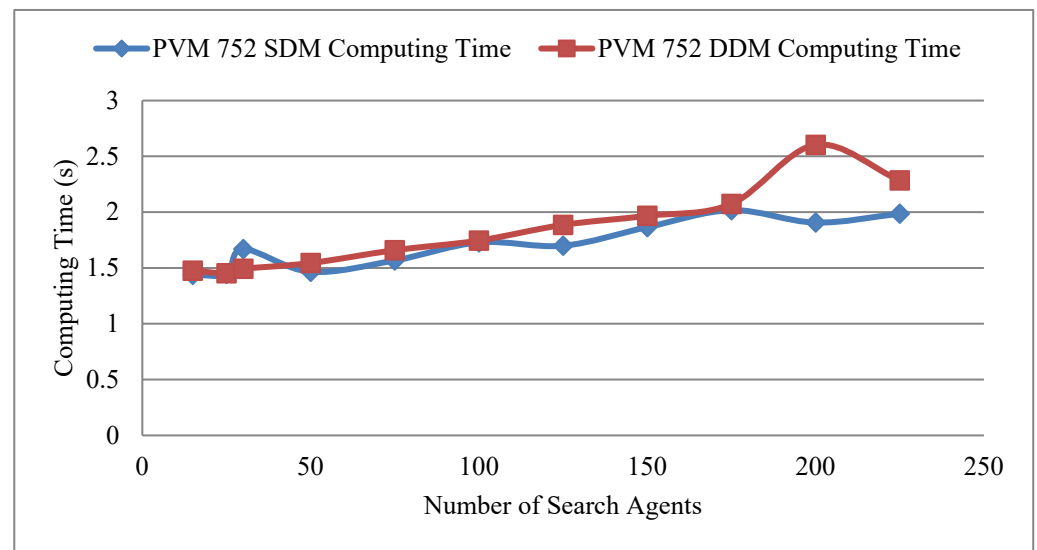
(**a**)
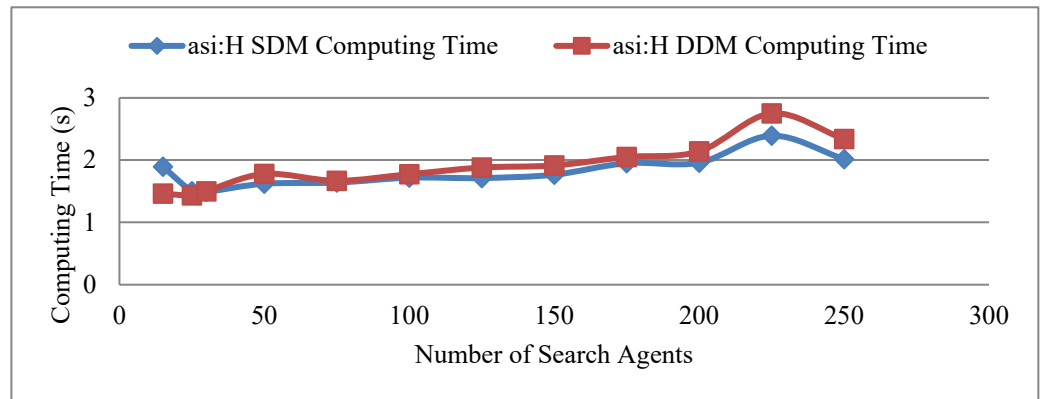


(**b**)
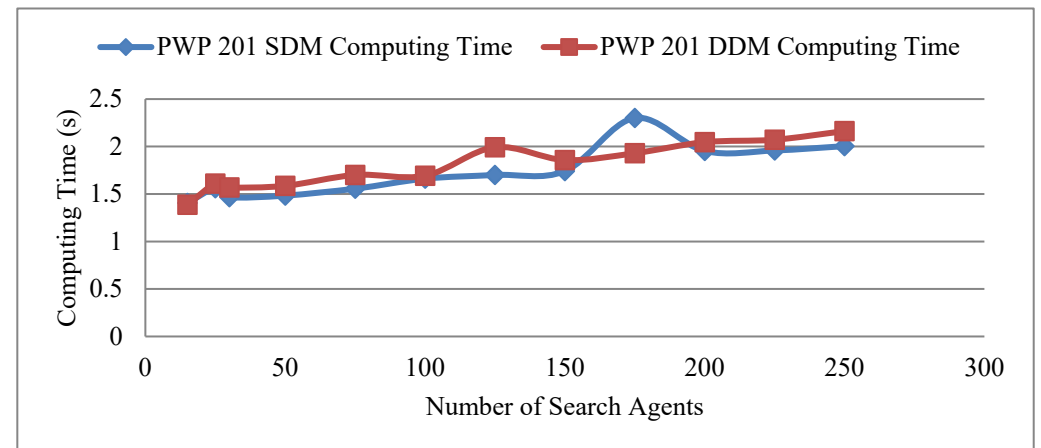


(**c**)

**Figure 15.** *Cont*.

(**d**)

**Figure 15.** BWOA computing time vs. the number of search agents (**a**) RTC cell, (**b**) aSi Cell, (**c**) PWP 201 panels, and (**d**) PVM 752 panel.

## 4. Conclusions

The main objective of this work is to improve the extraction of the two PV cells/panels (RTC, aSi, PVM 752 GaAs, and PWP 201) parameters for the single diode and double diodes models using the BWOA. Additionally, the proposed BWOA effectiveness is validated by comparing its results to those of various earlier optimization methods described in the literature.

The main conclusions are:

- BWOA yields lower values of statistical tests, such as RMSE, MRE, MBE, $R^2$, and $R_a^2$, in comparison with all algorithms considered;
- BWOA gives lower or the same results as RMSE. These vary from 0 to 3% for the SDM model and from 0.5% to 16.5% for the DDM model. The highest decrease is 16.5% for the PVM 752 GaAs in the DDM model;
- The proposed algorithm is accurate and rapidly extracts the PV cells/panels parameters. The computing time is very low, around 2 s;
- The analysis of the behavior of the RMSE, when the number of iterations varies, shows that the best results are obtained for 1500 iterations. In the case of the variation of the population sizes, the best solutions are obtained for more than 100. As for the analysis of the SDM and DDM models, when the population sizes vary, it does not show the model that would be expected, according to which a lesser number of parameters would mean it is possible to use a lesser population.

As a result, the suggested BWOA offers an alternative way for parameter extraction in PV cell/panel models.

The future research directions are to improve the algorithm's performance through hybridization and to apply the algorithm to extract the parameters of the triple diode model and multijunction photovoltaic cells for different conditions, such as different temperatures and irradiations (natural sunlight and in concentrated light up to 400 suns).

**Supplementary Materials:** The following supporting information can be downloaded at: https://www.mdpi.com/article/10.3390/math11040967/s1, Table S1. Dataset for RTC silicon photovoltaic cell and the results for the current using BWOA; Table S2. Dataset for aSi silicon photovoltaic cell and the results for the current using BWOA; Table S3. Dataset for PWP201 photovoltaic panel and the results for the current using BWOA; Table S4. Dataset for PVM 752 GaAs photovoltaic panel and the

results for the current using BWOA.; Table S5. RMSE and computing time function of the number of the search agents and iterations using the BWOA.

**Author Contributions:** Conceptualization, M.M. and D.T.C.; methodology, M.M., D.T.C. and P.A.C.; software, M.M.; validation, M.M., D.T.C. and P.A.C.; resources, M.M., D.T.C. and P.A.C.; writing— original draft preparation, M.M. and D.T.C.; writing—review and editing, M.M., D.T.C. and P.A.C. All authors have read and agreed to the published version of the manuscript.

**Data Availability Statement:** We present the data in the Supplementary Materials.

**Conflicts of Interest:** The authors declare no conflict of interest.

# References

1. Available online: https://ec.europa.eu/commission/presscorner/detail/en/ip_20_335 (accessed on 28 September 2022).
2. Chao, L.; Niu, T.; Gu, H.; Yang, Y.; Wei, Q.; Xia, Y.; Hui, W.; Zuo, S.; Zhu, Z.; Pei, C.; et al. Origin of High Efficiency and Long-Term Stability in Ionic Liquid Perovskite Photovoltaic. *Research* **2020**, *2020*, 1–13. [CrossRef] [PubMed]
3. Bagalini, V.; Zhao, B.Y.; Wang, R.Z.; Desideri, U. Solar PV-Battery-Electric Grid-Based Energy System for Residential Applications: System Configuration and Viability. *Research* **2019**, *2019*, 3838603. [CrossRef] [PubMed]
4. Cotfas, D.; Cotfas, P.; Kaplanis, S. Methods to determine the dc parameters of solar cells: A critical review. *Renew. Sustain. Energy Rev.* **2013**, *28*, 588–596. [CrossRef]
5. Humada, A.M.; Hojabri, M.; Mekhilef, S.; Hamada, H.M. Solar cell parameters extraction based on single and double-diode models: A review. *Renew. Sustain. Energy Rev.* **2015**, *56*, 494–509. [CrossRef]
6. Cotfas, D.T.; Cotfas, P.A.; Oproiu, M.P.; Ostafe, P.A. Analytical versus Metaheuristic Methods to Extract the Photovoltaic Cells and Panel Parameters. *Int. J. Photoenergy* **2021**, *2021*, 1–17. [CrossRef]
7. Yang, B.; Wang, J.; Zhang, X.; Yu, T.; Yao, W.; Shu, H.; Zeng, F.; Sun, L. Comprehensive overview of meta-heuristic algorithm applications on PV cell parameter identification. *Energy Convers. Manag.* **2020**, *208*, 112595. [CrossRef]
8. Li, S.; Gong, W.; Gu, Q. A comprehensive survey on meta-heuristic algorithms for parameter extraction of photovoltaic models. *Renew. Sustain. Energy Rev.* **2021**, *141*, 110828. [CrossRef]
9. Cotfas, D.T.; Deaconu, A.M.; Cotfas, P.A. Hybrid successive discretisation algorithm used to calculate parameters of the photovoltaic cells and panels for existing datasets. *IET Renew. Power Gener.* **2021**, *15*, 3661–3687. [CrossRef]
10. Xiong, G.; Zhang, J.; Shi, D.; He, Y. Parameter extraction of solar photovoltaic models using an improved whale op-timization algorithm. *Energy Convers. Manag.* **2018**, *174*, 388–405. [CrossRef]
11. Pourmousa, N.; Ebrahimi, S.M.; Malekzadeh, M.; Alizadeh, M. Parameter estimation of photovoltaic cells using improved Lozi map based chaotic optimization Algorithm. *Sol. Energy* **2019**, *180*, 180–191. [CrossRef]
12. Yu, K.; Liang, J.J.; Qu, B.Y.; Cheng, Z.; Wang, H. Multiple learning backtracking search algorithm for estimating pa-rameters of photovoltaic models. *Appl. Energy* **2018**, *226*, 408–422. [CrossRef]
13. Civicioglu, P. Backtracking Search Optimization Algorithm for numerical optimization problems. *Appl. Math. Comput.* **2013**, *219*, 8121–8144. [CrossRef]
14. Gomes, R.C.M.; Vitorino, M.A.; Correa, M.B.D.R.; Fernandes, D.A.; Wang, R. Shuffled Complex Evolution on Photovoltaic Parameter Extraction: A Comparative Analysis. *IEEE Trans. Sustain. Energy* **2016**, *8*, 805–815. [CrossRef]
15. Gao, X.; Cui, Y.; Hu, J.; Xu, G.; Wang, Z.; Qu, J.; Wang, H. Parameter extraction of solar cell models using improved shuffled complex evolution algorithm. *Energy Convers. Manag.* **2018**, *157*, 460–479. [CrossRef]
16. Cotfas, D.T.; Deaconu, A.M.; Cotfas, P.A. Application of successive discretization algorithm for determining photovoltaic cells parameters. *Energy Convers. Manag.* **2019**, *196*, 545–556. [CrossRef]
17. Madhiarasan, M.; Cotfas, D.T.; Cotfas, P.A. Barnacles Mating Optimizer Algorithm to Extract the Parameters of the Photovoltaic Cells and Panels. *Sensors* **2022**, *22*, 6989. [CrossRef]
18. Nunes, H.G.G.; Pombo, J.A.N.; Mariano, S.J.P.S.; Calado, M.R.A.; De Souza, J.F. A new high performance method for determining the parameters of PV cells andmodules based on guaranteed convergence particle swarm optimization. *Appl. Energy* **2018**, *211*, 774–791. [CrossRef]
19. Kler, D.; Sharma, P.; Banerjee, A.; Rana, K.; Kumar, V. PV cell and module efficient parameters estimation using Evaporation Rate based Water Cycle Algorithm. *Swarm Evol. Comput.* **2017**, *35*, 93–110. [CrossRef]
20. Xiong, G.; Zhang, J.; Shi, D.; Yuan, X. Application of Supply-Demand-Based Optimization for Parameter Extraction of Solar Photovoltaic Models. *Complexity* **2019**, *2019*, 1–22. [CrossRef]
21. Jiao, S.; Chong, G.; Huang, C.; Hu, H.; Wang, M.; Heidari, A.A.; Chen, H.; Zhao, X. Orthogonally adapted Harris hawks opti-mization for parameter estimation of photovoltaic models. *Energy* **2020**, *203*, 117804. [CrossRef]

22. Düzenli, T.; Onay, F.K.; Aydemir, S.B. Improved honey badger algorithms for parameter extraction in photovoltaic models. *Optik* **2022**, *268*, 169731. [CrossRef]

23. Abdollahzadeh, B.; Gharehchopogh, F.S.; Mirjalili, S. African vultures optimization algorithm: A new nature-inspired metaheuristic algorithm for global optimization problems. *Comput. Ind. Eng.* **2021**, *158*, 107408. [CrossRef]

24. El-Fergany, A.A. Parameters identification of PV model using improved slime mould optimizer and Lambert W-function. *Energy Rep.* **2021**, *7*, 875–887. [CrossRef]

25. Hamid, N.; Abounacer, R.; Oumhand, M.I.; Feddaoui, M.; Agliz, D. Parameters identification of photovoltaic solar cells and module using the genetic algorithm with convex combination crossover. *Int. J. Ambient. Energy* **2018**, *40*, 517–524. [CrossRef]

26. Lin, X.; Wu, Y. Parameters identification of photovoltaic models using niche-based particle swarm optimization in parallel computing architecture. *Energy* **2020**, *196*, 117054. [CrossRef]

27. Li, S.; Gu, Q.; Gong, W.; Ning, B. An enhanced adaptive differential evolution algorithm for parameter extraction of photo-voltaic models. *Energy Convers. Manag.* **2020**, *205*, 112443. [CrossRef]

28. Zhang, Y. Neural Network Algorithm with Reinforcement Learning for Parameters Extraction of Photovoltaic Models. *IEEE Trans. Neural Netw. Learn. Syst.* **2021**, 1–11. [CrossRef]

29. Zamani, H.; Nadimi-Shahraki, M.H.; Gandomi, A.H. Starling murmuration optimizer: A novel bio-inspired algorithm for global and engineering optimization. *Comput. Methods Appl. Mech. Eng.* **2022**, *392*, 114616. [CrossRef]

30. Zamani, H.; Nadimi-Shahraki, M.H.; Gandomi, A.H. QANA: Quantum-based avian navigation optimizer algorithm. *Eng. Appl. Artif. Intell.* **2021**, *104*, 104314. [CrossRef]

31. Chauhan, A.; Prakash, S. Comparison and performance analysis of pheromone value and cannibalism based black widow optimisation approaches for modelling and parameter estimation of solar photovoltaic mathematical models. *Optik* **2022**, *259*, 168943. [CrossRef]

32. Cotfas, P.; Cotfas, D. Design and implementation of RELab system to study the solar and wind energy. *Measurement* **2016**, *93*, 94–101. [CrossRef]

33. Hayyolalam, V.; Kazem, A.A.P. Black widow optimization algorithm: A novel meta-heuristic approach for solving en-gineering optimization problems. *Eng. Appl. Artif. Intell.* **2020**, *87*, 103249. [CrossRef]

34. Peña-Delgado, A.F.; Peraza-Vázquez, H.; Almazán-Covarrubias, J.H.; Torres Cruz, N.; García-Vite, P.M.; Morales-Cepeda, A.B.; Ramirez-Arredondo, J.M. A Novel Bio-Inspired Algorithm Applied to Selective Harmonic Elimination in a Three-Phase Eleven-Level Inverter. *Math. Probl. Eng.* **2020**, *2020*, 1–10. [CrossRef]

35. Easwarakhanthan, T.; Bottin, J.; Bouhouch, I.; Boutrit, C. Nonlinear Minimization Algorithm for Determining the Solar Cell Parameters with Microcomputers. *Int. J. Sol. Energy* **1986**, *4*, 1–12. [CrossRef]

36. Jordehi, A.R. Enhanced leader particle swarm optimisation (ELPSO): An efficient algorithm for parameter estimation of photo-voltaic (PV) cells and modules. *Sol. Energy* **2018**, *159*, 78–87. [CrossRef]